Bombay College of Pharmacy, Mumbai, India

Chitosan nanoparticles for controlled delivery of brimonidine tartrate to the ocular membrane

K. H. Singh, U. A. Shinde

Received October 22, 2010, accepted December 29, 2010

Dr. Ujwala Shinde, Department of Pharmaceutics, Bombay College of Pharmacy, Kalina, Santacruz (E), 400098 Mumbai, India
Ujwalashinde29@gmail.com

Pharmazie 66: 594–599 (2011) *doi: 10.1691/ph.2011.0349*

Various efforts have been made to improve the bioavailability and to prolong the residence time of eye drops. Drug loaded polymeric nanoparticles offer several favorable biological properties. Thus, brimonidine tartrate (BT) loaded chitosan (CS) nanoparticles were prepared by inducing the ionic gelation upon addition of sodium tripolyphosphate (TPP). Nanoparticles were characterized by TEM, SEM, particle size, polydispersity index (PI), DSC, IR, entrapment efficiency which gave an insight of physicochemical interaction that influenced the CS nanoparticle formation and entrapment of BT. *In vitro* release of BT nanoparticle showed sustained release over the period of 4 h in saline phosphate buffer pH 7.4. Both placebo and BT loaded nanoparticles had a mean particle size range of about 270-370 nm with PI less than 0.5. DSC studies demonstrated structural interactions between BT, TPP and CS matrix. Entrapment efficiency of the CS nanoparticles ranged from 36-49% depending on the CS:TPP weight ratio. *In vivo* studies confirmed a significant sustained effect of BT nanoparticles compared to conventional eye drops. These results suggest that BT loaded CS nanoparticles could help to reduce dosage frequency by sustained drug release in the treatment of glaucoma.

1. Introduction

The successful delivery of drugs into the eyes is extremely complicated since the eye is protected by a series of complex defense mechanism which make it difficult to achieve an effective concentration of drug within the target area of the eye. Pulse entry is another most common and yet highly undesirable problem with eye drops, as it results in initial high drug concentrations in the lachrymal fluid, followed by a rapid decline and thus suggests frequent dosing and potential risk of toxicity. Hence, to enhance the drug retention in the ocular *cul de sac*, it is essential to formulate drugs into innovative drug delivery systems.

New drug delivery systems, for the anterior segment of the eye includes ocular inserts, corneal shields and contact lenses, which provide controlled delivery of drug to the eye (Yasmin et al. 2006; Macha et al. 2003); *in situ* gelling systems, which provide ease of administration as drops and gets converted to gel form in the eye, thereby providing some sustained effect of drug in the eye, vesicular systems, offers advantages of targeted delivery, bio-compatibility and freedom from blurring of vision, mucoadhesive systems provides better retention in the eye (Annick 2005).

Particulate polymeric drug delivery systems include micro- and nanoparticles. After optimal drug binding to these particles, the drug absorption in the eye is enhanced significantly in comparison to eye drop solutions owing to the much slower elimination rates of the mucoadhesive particles (Kothuri et al. 2003).

Nanoparticles are colloidal drug carriers in the submicron range (10–1000 nm). These carriers have been evaluated for ophthalmic drug delivery purposes for the past 15 years. The main objective for these systems was to improve the classical aqueous eye drop formulations to combine ophthalmic prolonged action with the ease of application of eye drops. Drug loaded nanoparticles have been explored for its application in ophthalmic diseases like glaucoma, inflammations or infections of the eye (Nagarwal et al. 2009). Management of ocular diseases is mainly limited by the inability to provide long-term ocular drug delivery without avoiding the systemic drug exposure and/or affecting the intraocular structures and poor availability of drugs, which may be overcome by prolonging the contact time with the ocular surface, for instance with bioadhesive polymers (Sahoo et al. 2008).

Use of mucoadhesive polymers like Chitosan, result in attachment of polymeric particle to conjunctival mucin (a glycoprotein) via non-covalent bonds, thus remaining in contact with the precorneal tissues until mucin turnover causes elimination of the polymer. Their ability to localize a dosage form within a particular region which leads to optimum contact with the absorbing surface to permit modification of tissue permeability which prolonged residence time of drug, enhanced drug bioavailability and reduced dosing frequency (Alonso and Sánchez 2003).

Glaucoma is a group of diseases of the eye characterized by an increase in intraocular pressure (IOP) following damage to the ganglionic cells and the optic nerve. The increase in intraocular pressure associated with glaucoma is due to an increased resistance to the outflow of aqueous humor from the eye through the trabecular meshwork Schlemm's canal system.

Brimonidine tartrate is an α-agonist drug used in treatment of glaucoma and it appears to act by decreasing aqueous humor production and increasing aqueous outflow. Due to its selectiv-

Fig. 1: TEM of BT loaded CS nanoparticles

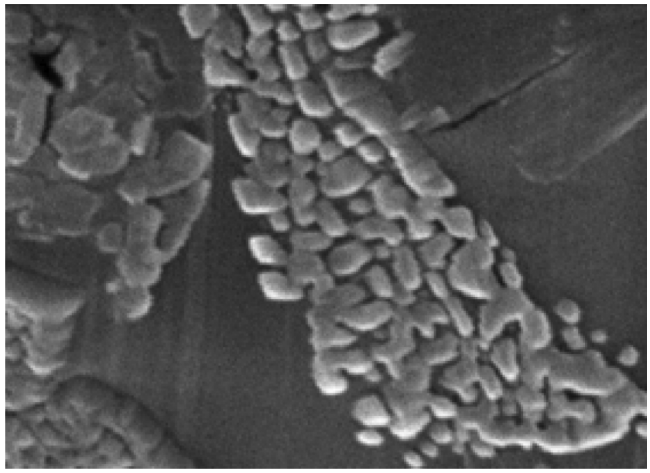

Fig. 3: SEM of BT loaded SA nanoparticles

ity for α receptors it has minimal cardiovascular or pulmonary effects after application to the conjuctiva (Soltau et al. 2002). Formulating brimonidine tartrate in a polymeric nanopaticulate form would provide combined benefits of aqueous solution formulation with reduced frequency of dosage (De et al. 2004). Brimonidine tartrate nanoparticulate carriers using CS, a bioadhesive polymer would be expected to not only reduce the pulse entry but also sustain the release of the drug in ocular *cul de sac*. Hence the study was planned to develop and evaluate brimonidine tartrate loaded chitosan nanoparticles to reduce the pulse entry and achieve sustained release of drug, which would result in reduction of dosing frequency and toxicity.

2. Investigations, results and discussion

2.1. Transmission electron microscopy and scanning electron microscopy

TEM of the BT-loaded SA nanoparticles showed that nanoparticles have a solid dense structure and they showed spherical shape as shown in Fig. 1. This may be attributed to the nucleation through ionic gelation followed by semi crystal formation and growth. TEM images showed the nanoparticles size ranges between 200–300 nm approximately which were found to be smaller than particle sizes determined by PCS. This discrepancy in size could be due to the dehydration of nanoparticles during sample preparation for TEM imaging (Motwani et al. 2008). Scanning electron photomicrographs (Figs. 2 and 3) revealed that the sharp crystalline structure of the BT was disappeared in nanoparticle pellet, which could be due to coating these crystals with CS.

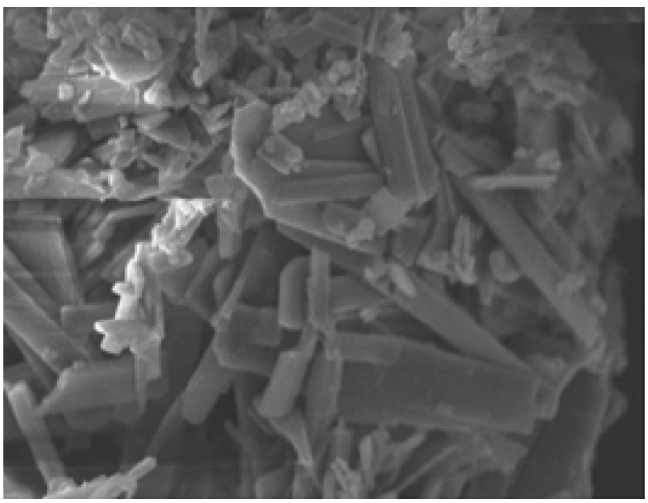

Fig. 2: SEM of BT drug crystals

2.2. DSC and FTIR analysis

DSC scans of plain BT powder, BT loaded CS nanoparticles and physical mixture of blank CS nanoparticles with BT drug powder are shown in Fig. 4. As clearly indicated in the DSC thermogram of the pure drug i.e. BT, drug showed a sharp endothermic peak at 210.36 °C, where as in the nanoparticles the characteristic peak of BT was shifted towards right i.e. at temperature 216.00 °C and the sharpness of the peak was reduced. When the DSC thermogram of the physical mixture of blank CS nanoparticles with the drug powder was taken, characteristic peak of BT crystal was observed without any significant shift and change in the peak intensity and peak value.

As indicated in the IR spectra characteristic peaks of BT such as 1599 (NH Bending), 1653(C=N & C=C stretching) & 1732 (C=O stretching) cm^{-1} were prominently masked in the BT loaded nanoparticles. Shift in the endothermic peak of DSC and change in peak intensity of IR spectrum was the indication of chemical and physical changes taking place through ionic gelation and nanoparticle formation process hence it can

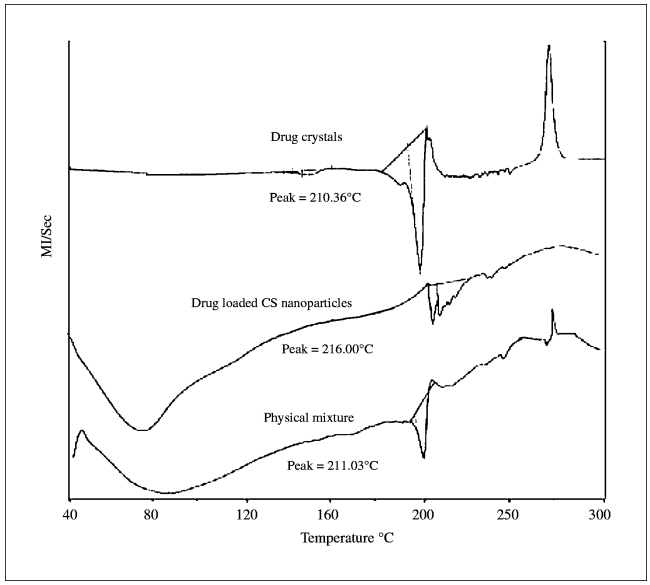

Fig. 4: DSC thermogram for BT, BT loaded CS nanoparticle, and physical mixture

Table 1: Effect of CS:TPP weight ratio on particle size, PI and visual appearance

CS: TPP	Particle size (μm)	P.I.	Visual appearance
1:1	17.507 ± 2.43	Optical microscopy	Opaque suspension
2:1	14.556 ± 1.95	Optical microscopy	Opaque suspension
3:1	12.217 ± 1.98	Optical microscopy	Opaque suspension
4:1	0.37026 ± 0.0051	0.396 ± 0.025	Clear transparent solution
5:1	0.3007 ± 0.0059	0.383 ± 0.021	Clear transparent solution
6:1	0.276 ± 0.0048	0.377 ± 0.030	Clear transparent solution

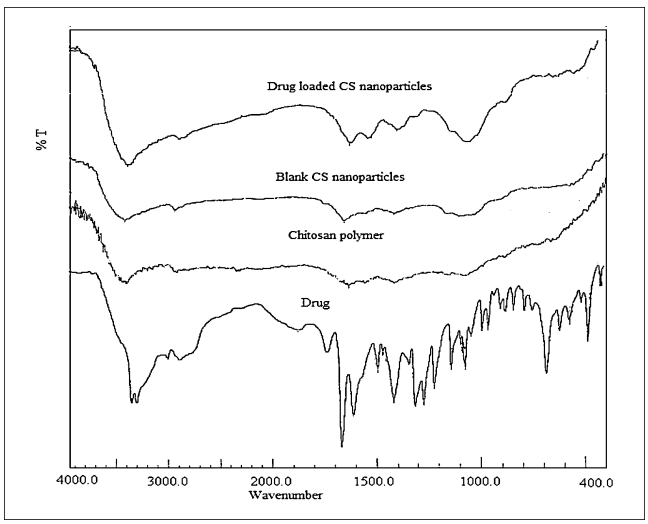

Fig. 5: IR spectra for BT loaded CS nanoparticle, blank nanoparticles, CS and BT

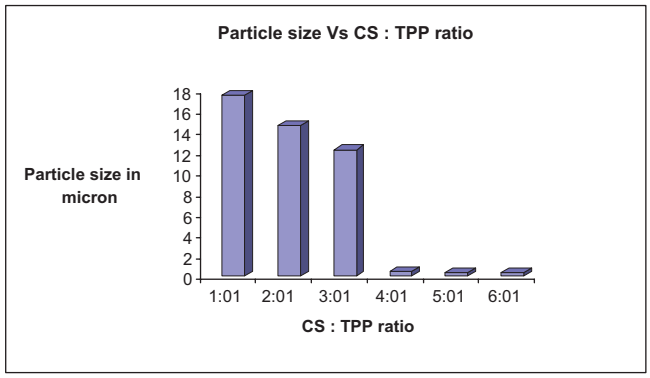

Fig. 6: Bar graph of CS:TPP weight ratio Vs Particle size in micron

be concluded that there was probable interaction between the protonated BT at the pH of preparation or positively charged ammonium group of CS and anionic tripolyphosphoric groups of TPP (Fig. 5).

2.3. Effect of CS:TPP weight ratios on the particle size, Zeta potential and % entrapment efficiency

Size and size distribution of CS nanoparticles depend largely on concentration of polymer and TPP. Hence CS nanoparticles were prepared by varying concentration of CS:TPP weight ratios and their effect on the particle size was investigated. The effect of CS:TPP weight ratio on particle size and P.I. has been shown in Table 1.

The weight ratio between CS and TPP is critical and controls the particle size and size distribution of the nanoparticles (Yaowalak et al. 2006). The size characteristics have been found to affect the biological performance of CS nanoparticles. Therefore, before the drug entrapment into CS nanoparticles, the effect of CS:TPP weight ratio on the size characteristics of the nanoparticles was studied in order to determine the optimum ratio which resulted in submicron particles with narrow particle size distribution range. During preparation of nanoparticles, when the TPP solution was added drop wise in aqueous CS solution, it was observed that the CS solution had turned into colloidal solution, opalescent solution and opalescent suspension as the concentration of TPP in the mixing ratio was increased. The changes in the particle size, PI and visual appearance for series of CS:TPP weight ratios revealed that as the concentration of TPP was increased, particle size and P.I. of nanoparticles was increased to give particles in micron range and viscosity of the formulation decreased. The increase in TPP concentration in the mixing ratio could lead to agglomeration of CS nanoparticles with excess anionic charge which resulted in increased particle size (Calvo et al. 1997). The optimum CS:TPP weight ratios which yielded particles in submicron range were found to be 4:1, 5:1 and 6:1.

The zeta potential of CS nanoparticles was obtained in order to determine the surface charge. The stability of the particles can be analyzed based on the zeta potential. Higher charge density on the particle surface produces repulsive interactions between particles. This leads to more uniform size distribution and also stability of the particles against aggregation effects and also on storage of nanoparticulate system (Chuanyun et al. 2005; Jerome et. al. 2007).

Table 2 represents the results of zeta potential of drug loaded nanoparticles. The average zeta potential of CS nanoparticles was +26.2 mV to +29.8 mV, which indicate that free (non cross-linked) cationic groups remained on the particle surface (http://www.pssnicomp.com/zetatheory.htm). These values indicate moderate stability of nanoparticles. The cationic surface charge of CS nanoparticles results in higher stability of particles in suspension through the electrostatic repulsion between particles (ASTM Standard D. 1985). The cationic charge of particles could also lead to the interaction of particles *in vivo* with the components of ocular mucin like sialic acid and other anions.

Table 2: Effect of CS:TPP weight ratios on the particle size, Zeta potential and % entrapment efficiency

CS:TPP weight ratio	Particle size in nm	Zeta potential in mV	% Entrapment efficiency
6:1	0.276 ± 0.0048	+ 29.8 ± 0.310	37.08 ± 3.20
5:1	0.3007 ± 0.0059	+ 28.5 ± 0.275	41.29 ± 2.75
4:1	0.37026 ± 0.0051	+ 26.2 ± 2.95	48.51 ± 2.65

Table 3: Effect of drug loading on percent entrapment efficiency

4:1; CS:TPP ratio with different drug loadings	% Entrapment efficiency
25 % Drug	46.17 ± 2.10
50 % Drug	48.54 ± 2.85
75 % Drug	48.97 ± 2.55

Zeta potential values were not markedly changed with change in CS:TPP weight ratio. Hence the zeta potential data for the BT loaded CS nanoparticles demonstrates that the system exhibits moderate stability.

2.4. Measurement of entrapment efficiency

The entrapment efficiency (EE) is the ratio of actual drug content in the nanoparticles to the theoretical amount of drug used for preparation of nanoparticles. Entrapment efficiency (EE) of BT in CS nanoparticles was estimated by an indirect method in which un-entrapped BT in supernatant was estimated.

The nanoparticles were formed due to electrostatic interaction between CS, TPP and BT. The pH of the CS solution was 5, at this pH BT possessed predominant positive charge due to protonation of amino group (pKa 7.4). Thus in principle protonated BT could develop ionic interactions with negatively charged TPP or CS nanoparticle having excess anionic charge on it (Motwani et al. 2008).

When anionic TPP was added to the solution of CS containing BT, ionic interaction was induced between positively charged CS, protonated BT and anionic TPP which resulted in the formation of nanoparticles which was confirmed in shift of endothermic peak in DSC analysis and change in peak intensity in FTIR.

The percent EE was found to be 37.08%, 41.29 % and 48.51 % as the concentration of TPP was increased from 6:1 to 4:1 in CS:TPP weight ratio, hence this ensured that concentration of TPP solution added had major effect on the entrapment efficiency. At high TPP concentration, CS nanoparticles produced had excess anionic charge which could have involved in ionic interaction with protonated BT. The increase in entrapment efficiency with increase in TPP concentration in CS:TPP ratio could be due to more intense ionic interaction between anionic TPP and cationic CS which indicate physical entrapment of the drug in nanoparticles. The possible ionic interaction between negatively charged CS nanoparticles and protonated BT results in electrostatic entrapment of drug in the nanoparticles.

For CS:TPP weight ratio 4:1, % EE was found to be maximum and the nanoparticles obtained with this ratio were in the submicron size range i.e. 359.10 ± 3.58 nm with PI 0.381 ± 0.032. Therefore, this ratio was further investigated for effect of drug loading. When CS:TPP weight ratio of 4:1 (ratio with highest entrapment efficiency) was loaded with different percentages of BT, there was no significant change in the entrapment efficiencies (Table 3). The entrapment of BT was not influenced by the BT concentration in the system but the key factor affecting the entrapment was CS:TPP weight ratio. The CS:TPP ratio with highest entrapment efficiency i.e. 4:1 was loaded with different drug concentrations (25% w/w, 50% w/w and 75% w/w) and evaluated for release profile.

2.5. In vitro drug release

The efficiency of an ocular dosage form is limited by its short residence time in culde sac, due to rapid elimination of drug from the corneal surface by lachrymal flow. Mucoadhesive polymer based drug delivery systems can be used for improving the drug retention and biodistribution for topical ocular application. To overcome this limitation, ocular administration of the drugs in the nanoparticle form has been reported in the literature. CS nanoparticles being in submicron size range and mucoadhesive, could not only improve drug residence times but also offer the advantage of patient compliance. The *in vitro* release profiles of BT loaded CS nanoparticles prepared with varying CS:TPP weight ratios were studied in saline phosphate buffer pH 7.4. The *in vitro* release profiles of BT nanoparticles were compared with release of BT from its aqueous solution. The values of $t_{50\%}$ release (Fig. 7) for BT solution were 30 min. BT nanoparticles varying CS:TPP ratio required time for 50% drug release as 60 min for ratio 4:1 and 5:1 and 85 min for 6:1 ratio. These values revealed that BT in nanoparticulate form can be effectively sustaining BT release.

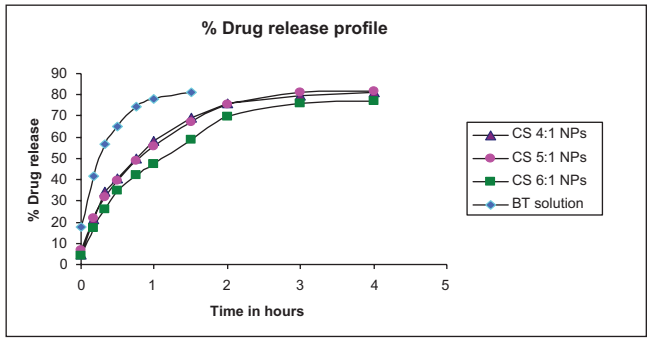

Fig. 7: Percent drug release vs. time in hours

The release of the BT from CS nanoparticles followed a biphasic pattern, characterized by initial burst release followed by a prolonged release. The burst release lasted for 45 min, and during this period 40 to 45% drug release was observed. This initial burst release was due to unentrapped drug in nanoparticle formulation which can have advantage of providing immediate dose available for reducing the IOP and after 45 min release was sustained over the period of 4 h. Initial burst release could be due to rapid dissolution of BT nano-crystals associated with surface of CS nanoparticles which was confirmed in scanning electron photomicrographs. In addition, the large surface area that characterizes nanoparticles can adsorb the drug, so the burst release is possibly due to the part of BT desorbed from nanoparticles surface. After the initial burst release period, the rate of release was reduced which could be attributed to slow diffusion of the drug through matrix of CS nanoparticles.

2.6. In vivo studies

Draize eye test is a well established test used for evaluation of safety of ocular product, it allows assessment of the potential ophthalmic hazard of a substance, and the test is proposed to grade the extent of eye injury due to the formulation in the albino rabbits.

Eyes were checked for any immediate reaction (erythema, edema, lachrymation etc.) and also at intervals of 1 h, 24 h and 48 h. No redness or sign of irritation was observed after instillation of the BT nanoparticles; hence eye irritation study ensured that the developed nanoparticulate system of CS was found to be safe on ocular instillation. The pharmacodynamic evaluation is presented as the change in IOP (ΔIOP) vs time in Fig. 8.

Instillation of a marketed formulation of BT (alphagan® P) showed peak after 2 h and declined rapidly within 5 h. In case of BT loaded CS nanoparticles the onset of action started within 30 min, showed a peak at the 5th h and a significant effect was observed for up to 8 h. When compared with Alphagan®P, a bet-

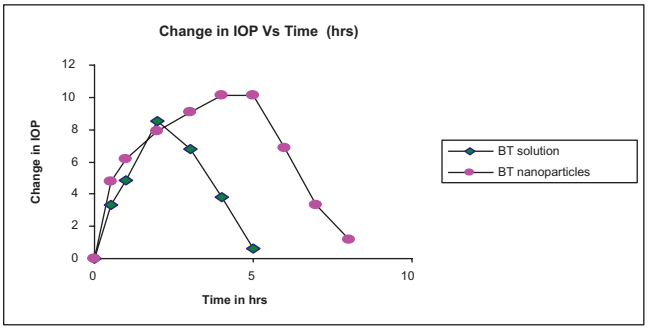

Fig. 8: Change in IOP v/s time

Table 4: Δ IOP (mm Hg) at various time intervals (h) for different formulations of BT

Time	Control	CS nanoparticles	BT solution
0 h	0	0	0
0.5 h	–0.13 ± 0.06	−4.80 ± 1.57***	−3.33 ± 1.66*
1 h	–0.17 ± 0.06	–6.20 ± 1.54**	–4.87 ± 1.58**
2 h	–0.23 ± 0.06	–7.93 ± 1.87**	–8.50 ± 1.80**
3 h	–0.23 ± 0.06	–9.10 ± 1.85**	–6.80 ± 2.41**
4 h	–0.27 ± 0.06	–10.17 ± 1.83***	–3.83 ± 4.01
5 h	–0.33 ± 0.06	–10.10 ± 1.87***	–0.60 ± 1.04
6 h	–0.33 ± 0.06	–4.83 ± 1.75*	0
7 h	–0.23 ± 0.06	–3.30 ± 1.61*	0
8 h	–0.23 ± 0.06	–1.17 ± 1.01	0

ter control of IOP was observed for BT loaded nanoparticles at times ≥ 5 h.

The lowering of IOP in the control eye was possibly due to the systemic absorption of BT upon topical instillation into the treated eye. It has been reported that CS effectively interacts with components of the mucus membrane in the body in order to provide a mucoadhesive coating (Banning et al.). The interaction of CS with mucin provides an effective mucoadhesive coating and prolongs the release of drug from the nanoparticulate formulation. As shown in the Table 4 developed nanoparticulate formulations of CS showed statistically significant response when compared to the control group because the p value was less than 0.05 for all the time points from 0.5 h to 7 h. The standard formulation i.e. BT solution was found to be statistically significant only for 0.5 h, 1 h, 2 h and 3 h.

2.7. Freeze drying and redispersibility of nanoparticles

Physical stability of the nanoparticle formulations was assessed by evaluating particle size, PI measurement and *in vitro* release study over a period of 5 weeks, was found to be stable with respect to particle size and percent drug release at the end of each week (Table 5).

The particle size of BT loaded nanoparticle was found to increase from 359.10 nm with PI 0.381 to 427.2 nm with PI 0.510 and *in vitro* release profile was not significantly changed for reconstituted freeze dried sample. Percentage of drug released at the end of 4 h was found to be similar before and after freeze drying.

3. Experimental

3.1. Chemicals

Chitosan (CS) was provided by the Central Institute of Fisheries Technology, Kochi (CIFT), India. Brimonidine tartrate (BT) was a gift from Cipla Ltd (India). Sodium tripolyphosphate (TPP) was purchased from Sigma-Aldrich. Other materials were analytical grade chemicals.

3.2. Preparation of Chitosan nanoparticles

Various methods are reported for the preparation of CS nanoparticles. Ionotropic gelation is the most convenient technique reported for CS nanoparticle preparation. It involves a limited number of processing steps and the use of conventional stirring equipment (magnetic stirrer) (Vauthier and Bouhemal 2009).

In the present study, CS nanoparticles were prepared by ionotropic gelation method, which was induced by adding 1% w/v TPP solution to the solution of CS with stirring. Briefly, the purified CS was dissolved in glacial acetic acid to prepare solution of 4 mg/ml concentration. The pH of CS solution was adjusted to 5.5 with sodium acetate buffer and 1 M sodium hydroxide. CS nanoparticles were formed spontaneously at room temperature when 1% w/v TPP solution was added at the rate 0.1 ml/min to the aqueous solution of CS under magnetic stirring. After complete addition of TPP solution, solution was further stirred for 30 min to ensure complete gelation of nanoparticles. Nanoparticulate batches (10 ml) were prepared by varying the concentration of CS and TPP in weight ratio such as 1:1, 2:1, 3:1, 4:1, 5:1 and 6:1. Drug loaded nanoparticles were prepared by dissolving BT in CS solution and 1% TPP solution was added dropwise as described for blank nanoparticles (Calvo et al. 1997).

Different drug concentrations were used in order to study the effect of the drug loading on the particle size, entrapment efficiency and *in vitro* release study. Non-entrapped drug was removed by ultracentrifugation at 30,000 × g for 45 min and pellets were evaluated for morphological and physicochemical characteristics. The supernatant was further analyzed for drug content. Every sample was prepared in triplicate and represented the average value. SD was calculated. The final optimized drug loaded nanoparticles were freeze dried (Papadimitriou et al. 2008).

3.3. Characterization of Chitosan nanoparticles

3.3.1. Morphology and surface topography of nanoparticles

Transmission electron microscopy (TEM) was used to examine the morphology of the BT loaded nanoparticles. TEM micrographs were obtained with a Philips CM-200 (Philips, Netherland) transmission electron microscope; wherein a sample drop was pretreated with colloid coated copper grid and left for 10 min to allow some of particles to adhere to collodion. The excess remaining dispersion was drawn off with filter paper. A drop of 2% aqueous uranyl acetate was applied for 1 min. The excess was then removed and sample was air dried and examined.

The surface topography of dry pellet of BT nanoparticles was studied with scanning electron microscopy. Pellets were coated using JEOL Ion sputter with thin layer of gold. Images were recorded on Jeol JSM-840 (Jeol Ltd, Tokyo, Japan) scanning electron microscope.

3.3.2. Differential scanning calorimetry analysis

Differential scanning calorimetry (DSC) analysis was used to characterize the thermal behavior and any possible interaction occurred between CS, TPP and BT during nanoparticle preparation. DSC thermograms of drug, BT nanoparticles were obtained using a Perkin-Elmer Pyris 1 DSC, equipped with Intracooler 2P cooling accessory. The instrument was operated under N_2 purge gas, samples (5 mg) were weighed in aluminium pans and heated at scanning rate of 10 °C/min and DSC scans were recorded over the temperature ranging from 0 to 300 °C.

3.3.3. FTIR analysis

FTIR spectroscopy has been successfully used for exploring the differences in molecular conformations, crystal packing and hydrogen bonding arrangements for different solid-state forms of an organic compound. The

Table 5: Physical stability of the BT loaded CS nanoparticles in 5 weeks

Time points	Particle size (nm)	Polydispersity index	pH
0	435.2 ± 3.98	0.423 ± 0.067	5.20
1 week	472.8 ± 8.32	0.497 ± 0.029	5.40
2 week	493.1 ± 6.73	0.501 ± 0.032	5.50
3 week	515.3 ± 9.61	0.623 ± 0.045	5.50
4 week	556.5 ± 10.22	0.679 ± 0.051	5.60
5 week	587.4 ± 10.51	0.712 ± 0.063	5.60

infrared spectra of BT, blank nanoparticles and BT loaded nanoparticles were recorded on a Jasco FT/IR 5300 spectrophotometer by preparing potassium bromide (KBr) pellets containing the samples.

3.3.4. Measurement of particle size and zeta potential

Nanoparticle size was determined by photon correlation spectroscopy (PCS), using a Beckman Coulter N5 plus Submicron Particle Sizer (Coulter Corporation, USA). To ensure light scattering intensity within instrument's sensitivity range, the samples were diluted with distilled water previously filtered through 0.45 micron membrane filter. For the determination of electrophoretic mobility nanoparticle samples were diluted with 0.1 mm KCl and placed in the electrophoretic cell, where a potential of 150 mV was established and zeta potential was measured in triplicate by Zetasizer Nano-ZS, UK.

3.4. Measurement of entrapment efficiency of brimonidine tartrate

For the determination of the entrapment efficiency, the nanoparticles were first separated from the aqueous suspension medium by ultracentrifugation at 30000 × *g* for 45 min. The amount of free BT in supernatant was measured by validated UV spectrophotometric method at 319 nm. The BT entrapment efficiency (EE) of nanoparticles was determined in triplicate and calculated by the difference the total amount used to prepare BT loaded nanoparticles and the amount of free BT determined in the supernatant (Alonso and Sánchez 2003).

3.5. In vitro release studies

Aliquot of the suspension of nanoparticles equivalent to 2.0 mg/ml of BT was placed in dialysis bags with molecular weight cut off between 12KD to 14KD, tied and placed in the 100 ml saline phosphate buffer pH 7.4 (PBS). At different time intervals, 5 ml dissolution samples were withdrawn and replaced with the fresh PBS. BT release was evaluated by UV spectrophotometric method at 319 nm. The entire system was kept at $37 \pm 0.5\,^{\circ}C$ with continuous magnetic stirring. To evaluate sustained release potential of mucoadhesive BT loaded CS nanoparticles, the *in vitro* release profiles of 0.2%w/v BT solution was also determined under similar condition and considered as reference.

3.6. In vivo studies

A freshly prepared sterile nanoparticles equivalent to 2.0 mg/ml BT and marketed preparation alphagan®P (brimonidine tartrate ophthalmic solution) containing an equivalent amount of BT was taken for the *in vivo* efficacy evaluation. Procedures were confirmed to the CPCSEA resolution on use of animals in research before commencement of experiment. Animals were allowed to move freely, their eye movements were not restricted. Studies were performed on fully-awake female New Zealand rabbits 2.0–2.5 kg, free from signs of ocular inflammation or gross abnormalities.

3.6.1. Draize test

Modified Draize test has been used to assess and evaluate the toxic characteristics of a formulation (Kirk et al. 2001). The eyes were checked for any abnormalities prior to the studies. The samples are placed in one eye keeping the other eye as control and the samples were instilled into one eye of the rabbit by gently pulling the lower lid away from the eyeball to form a cup whereas other eye of rabbit was kept as control. The lids were then gently held together for 10 s and then released. The time was recorded and eyes were checked for any immediate reaction (erythema, edema, lachrymation etc.) and also at intervals of 1 h, 24 h and 48 h (Ballantyne 1993).

3.6.2. Efficacy study (Acute measurement of intraocular pressure)

Adult male normotensive rabbits weighing 1.5–2.0 kg were used for the *in vivo* pharmacodynamic studies. Change in IOP
(Δ IOP) for each eye was determined as follows.

$$\Delta\text{IOP} = \text{IOP}_{\text{zero time}} - \text{IOP}_{\text{time't'}}$$

It is based upon the principle of measuring the change in the intraocular pressure after application of the formulation in eye of albino rabbits (White New Zealand rabbits) (Schultz and Vogel 2002)**.**
Before taking the readings, lignocaine solution 2%w/v was instilled into the rabbit's eye for anesthetizing the eye. Followed by anesthetization, formulation was placed in the cul-de-sac of one eye of animals keeping the other eye as control and response was recorded in triplicates. At different times intraocular pressure was measured with a hand held tonometer (Schioetz tonometer, germany) at following time intervals 0.5 h, 1 h, 2 h, 3 h, 4 h, 5 h, 6 h, 7 h and 8 h. The same steps were followed for the marketed formulation to obtain the drug response.

Results were treated with Student't' test to determine the level of significance. The statistical significance of the differences between BT nanoparticle formulation and the corresponding controls was tested, at each time point intervals with the pair wise multiple comparison procedure (student't, test) for multiple comparison. Differences were considered to be significant at a level of $P < 0.05$.

3.7. Freeze drying and redispersibility of nanoparticles

The physical stability of BT loaded CS nanoparticles was assessed over the period of 5 weeks. Nanoparticle formulations were freeze dried to study the stability of dried nanoparticles and nanoparticle suspension following redispersion. Mannitol 15% w/v was added as cryoprotectant to 10 ml aliquots of samples which were frozen in liquid nitrogen and lyophilized for 48 h. Freeze dried samples were stored at RT, were rehydrated to original volume by adding filtered distilled water. Reconstituted samples were assessed for particle size, PI and *in vitro* release.

Acknowledgement: Authors are thankful to Tata Institute of Fundamental Research, Mumbai, India for carrying out SEM and DSC analysis.

References

Alonso MJ, Sánchez A (2003) The potential of chitosan in ocular drug delivery. J Pharm Pharmacol 55: 1451–1463.

Annick L (2005) The use of mucoadhesive polymers in ocular drug delivery. Adv Drug Deliver Rev 57: 1595–1639.

ASTM Standard D (1985) Zeta Potential of Colloids in Water and Waste Water. 4187–82.

Ballantyne B (1993) Ophthalmic Toxicology. In: Ballantyne B, Mars T, Turner P (ed.) General And Applied Toxicology. 1st ed., Lancaster, pp. 504–519.

Banning D, Dettmar PW, Jolliffe IG, Hampson FC, Onsoyen EJ, Field PF, Craig D, Quinell M, Kristensen AH. (2007) US Patent No. 6395307.

Calvo P, Remuñán-López C, Vila-Jato JL, Alonso MJ (1997) Novel hydrophilic chitosan-polyethylene oxide nanoparticles as protein carriers. J Appl Polym Sci 63: 125–132.

Chuanyun D, Bochu W, Hongwei Z (2005) Microencapsulation peptide and protein drugs delivery system. Colloid Surface B 41: 117–120.

De TK, Bergey EJ, Chung SJ, Rodman DJ, Bharali DJ, Prasad PN (2004) Polycarboxylic acid nanoparticles for ophthalmic drug delivery: an *ex vivo* evaluation with human cornea. J Microencapsul 21: 841–855. http://www.pssnicomp.com/zetatheory.htm.

Kirk RW (2001) Draize test. Surv Ophthalmol 45: 493–515.

Kothuri MK, Pinnamaneni S, Das NG, Das SK (2003) Microparticles and nanoparticles in ocular drug delivery. In: Ashim K Mitra (ed.) Opthalmic Drug Delivery Systems. 2nd ed., New York, p. 437–466.

Macha S, Hughes PM, Mitra AK (2003) Overview of Ocular Drug Delivery. In: Ashim K Mitra (ed.) Ophthalmic Drug Delivery Systems. 2nd ed., New York, p 1–11.

Motwani SK, Chopra S, Talegaonkar S, Kohli K, Ahmad F J, Khar R K (2008) Chitosan–sodium alginate nanoparticles as submicroscopic reservoirs for ocular delivery: Formulation, optimization and *in vitro* characterization. Eur J Pharm Biopharm 68: 513–525.

Nagarwal RC, ShriKant, Singh PN, Maiti P, Pandit JK (2009) Polymeric nanoparticulate system: A potential approach for ocular drug delivery. J Control Release 136: 2–13.

Papadimitriou S, Bikiaris D, Avgoustakis K, Karavas E, Georgarakis M (2008) Chitosan naoparticles loaded with dorzolamide and pramipexole. Carbohyd Polym 73: 44–54.

Rose J, Thill A, Brant J (2007) Method for Structural and Chemical Characterization of Nanomaterials. In: Wiesner MR, Bottero J (ed.), Environmental Nanotechnology, 1st ed., New York, p. 144.

Sahoo S. K, Krishnakumar S, Dilnawaz F (2008) Nanotechnology in ocular drug delivery. Drug Discov Today 13: 144–151.

Schultz B, Vogel WH (2002) Ophthalmologic activity. In: HG Vogel (ed.) Drug Discovery and Evaluation: Pharmacological Assays. 2nd ed., New York: 1295–1297.

Soltau JB, Zimmerman TJ (2002) Changing Paradigms in the Medical Treatment of Glaucoma. Surv Ophthalmol. 47: S2-S5.

Vauthier C, Bouhemal K (2009) Methods for the Preparation and Manufacture of Polymeric Nanoparticles. Pharm Res 26: 1025–1058.

Yaowalak B, Ampol M, Müller BW (2006) Chitosan drug binding by ionic interaction. Eur J Pharm Biopharm. 62: 267–274.

Yasmin S, R Jain, M Aqil, Asgar A (2006) Review of ocular drug delivery. Curr Drug Deliv 3: 207–217.